

Numerical simulation of 2D crack growth with frictional contact in brittle materials

Kai Zhang.^{1,2,3} Qing Yang.^{1,3} Jing-Cai Jiang.²

¹School of Civil Engineering, Dalian University of Technology, China;

²Faculty of Engineering, The University of Tokushima, Japan;

³The State Key Laboratory of Coastal and Offshore Engineering, Dalian University of Technology, China

ABSTRACT: In this paper, the extended finite element method (XFEM) is applied in modeling the 2D crack growth with frictional contact under uniaxial compress load in the rock-like materials. First, the implementation of XFEM is incorporated into a commercial FEM software (ABAQUS) in which the constitutive law of linear elasticity and the criterion of maximum tangential stress (MTS) is adopted. Then a user subroutine is coded and incorporated into ABAQUS to simulate the growth of wing crack with the frictional contact in the crack faces. A series of numerical simulations of 2D plane strain rectangle with central pre-set crack are carried out, and computed results are compared with experimental ones. The effects of inclination and coefficient of the friction of the pre-set cracks on growth of wing cracks are examined. In addition, size effect of materials is also investigated, and these jobs contribute to the understanding of 2D crack growth.

Keywords: Extended finite element method (XFEM); Rock-like materials; Crack growth; Frictional contact; Size effect

1. INTRODUCTION

The discontinuities (e.g. joint, crack, and void) which exist previously or appear during the evolution often control the instability and final failure in the brittle materials. In recent years, a lot of experiments and numerical simulations have been carried on crack growth in brittle materials, such as rock, concrete and so on. It has been widely acknowledged that FEM is one of the effective methods used to model the crack problem because of its good adaptability and scalability. But conventional FEM has many difficulties in dealing with the strong discontinuities, which mostly lead to high density meshes on the crack tip or repeated remeshing as crack grows [1].

The Extend Finite Element Method (XFEM) originally proposed by Belytschko and Black [2, 3] in 1999, is very powerful for discontinuous problems in fracture mechanics. They added discontinuous enrichment function to the finite element approximation to account for the presence of the crack. Later, other researchers improved the method, and applied it in many subjects in fracture mechanics.

Actually, the extended finite element method (XFEM) is an extension of the conventional finite element method based on the concept of partition of unity. It allows the presence of discontinuities in an element by enriching degrees of freedom with special displacement functions. It does not require the mesh to match the geometry of the discontinuities. It allows contact interaction of cracked element surfaces based on a small-sliding formulation and allows both material and geometrical nonlinearity [4].

During the numerical analysis, the contact is a typical nonlinear problem, which not only due to the complicated mechanical model for the contact surface, but also more originate from the special discontinuous constraint of contact surface. The convergent results are difficult to

obtain only when the appropriate friction model is chosen. In the simulation of the paper, the penalty method is used to deal with the frictional contact of the crack surfaces during the load process, which can better model the impact on the contact surface when the wing crack grows.

This paper intends to contribute to the understanding of 2D crack growth under uniaxial compress load in brittle material with frictional contact, and a series of numerical modeling are carried out whose results are compared with experimental ones [5]. The effects of inclination and coefficient of the friction of the pre-set cracks on growth of wing cracks are examined.

2. THE XFEM APPROXIMATION

In the classical FEM, the approximation to displacement field $u(x)$ is expressed as [1]

$$\mathbf{u}^h(x) = \sum_{i=1}^n N_i \mathbf{u}_i \quad (1)$$

where N_i is the interpolated shape function associate with the node i ; \mathbf{u}_i is the classical vectorial DOF(degrees of freedom) at node i . For each computational point (x, y) in the field, N_i should satisfy PU (partition of unit):

$$\sum_{i=1}^{n^e} N_i(x, y) \equiv 1. \quad (2)$$

The XFEM enriched a standard approximation locally on the crack with discontinuous functions.

$$\begin{aligned} \mathbf{u}^h(\mathbf{x}) = & \sum_{i \in I} N_i(\mathbf{x}) \mathbf{u}_i + \sum_{j \in J} H(x) N_j(\mathbf{x}) \mathbf{a}_j \\ & + \sum_{k \in K_1} N_k(\mathbf{x}) \left(\sum_{l=1}^4 \mathbf{b}_k^{l1} \varphi_l^1(r, \theta) \right) + \sum_{k \in K_2} N_k(\mathbf{x}) \left(\sum_{l=1}^4 \mathbf{b}_k^{l2} \varphi_l^2(r, \theta) \right) \end{aligned} \quad (3)$$

where I is the set of all nodes in the mesh; J is the subset of nodes which support is intersected by the crack but do not cover any crack tips (e.g. the circled nodes in Fig. 1.); K_1, K_2 is the subset of nodes which support conclude the first and second crack tips (e.g. the squared and diamond nodes in Fig. 1).

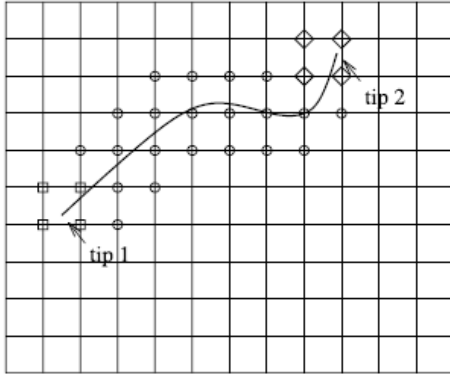


Fig. 1 An arbitrary crack placed on a mesh

The function $H(x)$ is a “generalized Heaviside” function, in which the discontinuity is aligned with the crack surface Γ_d . \mathbf{a}_j is the corresponding additional DOF for the discontinuity. Given a point in the domain, we denote the vectorial distance $\Delta \mathbf{x}$ between it and the closet point on Γ_d . Also, the normal vector to Γ_d is constructed. The function $H(x)$ is then given by the sign of the scalar product $\Delta \mathbf{x} \cdot \mathbf{e}_n$:

$$H(x) = \text{sign}(\Delta \mathbf{x} \cdot \mathbf{e}_n) = \begin{cases} 1, \Delta \mathbf{x} \cdot \mathbf{e}_n > 0, \\ -1, \Delta \mathbf{x} \cdot \mathbf{e}_n < 0. \end{cases} \quad (4)$$

The set of near-tip functions $\phi_l(r, \theta)$ are a set of additional shape functions which span the exact asymptotic crack-tip fields for a linear elastic material:

$$\{\phi_l(r, \theta)\} = \left\{ \sqrt{r} \sin\left(\frac{\theta}{2}\right), \sqrt{r} \cos\left(\frac{\theta}{2}\right), \sqrt{r} \sin\left(\frac{\theta}{2}\right) \sin(\theta), \sqrt{r} \cos\left(\frac{\theta}{2}\right) \sin(\theta) \right\} \quad (5)$$

where (r, θ) are the local polar coordinates at the crack tip. Except this, b_k^l is corresponding additional DOF for the crack tip.

3. FRICTIONAL BEHAVIORS

3.1 Conventional friction theories

Usually, when the inner surfaces of the crack are in contact, the shear force will be transmitted as well as the normal force across the interface. We now consider unilateral contact with friction on the interface.

The crack faces or the interface are assumed as $\Gamma_d = \Gamma_d^- \cup \Gamma_d^+$ with the unit normal vector to Γ_d^+ denote by \mathbf{n} in Fig. 2, and in the later modeling flat ellipse is

chosen which is close to the real situation of rock-like material. We also introduce the displacement and traction on each face of the crack: $\mathbf{w}^-, \mathbf{t}^-$ on Γ_d^- and $\mathbf{w}^+, \mathbf{t}^+$ on Γ_d^+ [6].

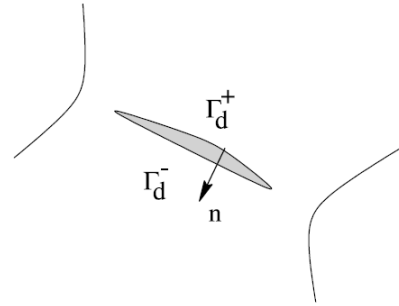


Fig. 2 The crack faces

The frictional model is easily described by using the appropriate form of the displacement and traction on the crack faces. The normal components are expressed in the condition of no contact and in contact:

$$(\mathbf{w}^- - \mathbf{w}^+) \cdot \mathbf{n} \geq 0, \quad (6A)$$

$$\mathbf{t}^+ \cdot \mathbf{n} \leq 0, \mathbf{t}^- \cdot \mathbf{n} \geq 0, \mathbf{t}^+ \cdot \mathbf{n} = -\mathbf{t}^- \cdot \mathbf{n}, \quad (6B)$$

$$(\mathbf{t}^+ \cdot \mathbf{n})(\mathbf{w}^- - \mathbf{w}^+) \cdot \mathbf{n} = 0 \quad (6C)$$

The tangential component will satisfy the equilibrium:

$$\mathbf{n} \times (\mathbf{t}^+ \times \mathbf{n}) + \mathbf{n} \times (\mathbf{t}^- \times \mathbf{n}) = \mathbf{0}, \quad (7)$$

so that the standard value of the tangential component can be represented by

$$p = \|\mathbf{n} \times (\mathbf{t}^+ \times \mathbf{n})\|. \quad (8)$$

The additional equations depend on whether or not there is friction. When the friction is idealized using a Coulomb law, two contacting surfaces can carry shear stress up to the maximum frictional force before they start sliding relative to each other:

$$g = \mu |\mathbf{t} \cdot \mathbf{n}|, \quad (9)$$

where μ is the coefficient of friction.

There is two states (sticking and sliding) and two equations to be satisfied are:

$$\mathbf{n} \times (\mathbf{w}^+ \times \mathbf{n}) = \mathbf{n} \times (\mathbf{w}^- \times \mathbf{n}) \quad \text{if } p < g \text{ (stick),} \quad (10A)$$

$$\mathbf{n} \times (\mathbf{w}^+ \times \mathbf{n}) - \mathbf{n} \times (\mathbf{w}^- \times \mathbf{n}) \neq 0 \quad \text{if } p = g \text{ (slide).} \quad (10B)$$

3.2 Stiffness method for friction

The stiffness method used for friction is a penalty method that permits some relative motion for the surfaces called elastic slip when they should be sticking. While the surfaces are sticking, the magnitude of sliding is limited to the elastic slip and adjusted to enforce this condition.

The stiffness method requires the appropriate selection of an allowable elastic slip γ_i . Using a larger γ_i makes the convergence of the solution more rapid, but brings the bad accuracy. If γ_i is chosen very small, convergence problems may occur. So the value of allowable slip used in the simulation which works very well must provide a conservative balance between efficiency and accuracy.

The allowable elastic slip is given as [4]

$$\gamma_i = F_f \bar{l}_i \tag{11}$$

where F_f is the slip tolerance, and \bar{l}_i is the characteristic contact surface length.

4. NUMERICAL EXAMPLES

4.1 The pre-set of parameters

The models used in the numerical study are rectangle blocks with dimension 240 mm high and 120 mm wide. A pre-existing flaw (25 mm long and 0.5 mm wide) with different inclinations and coefficients of friction is set up in the center of each model (Fig. 3). The flaw will close during the loading procedure. The other parameters of the flaw and the parameters of the material see Table 1 and Table 2.

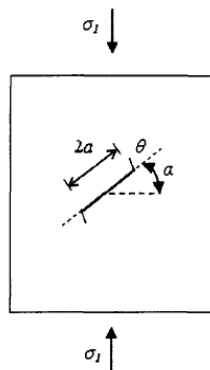


Fig. 3 The model of a flaw under compression (2a: the length of the flaw, θ : the initial angle)

Table 1 The dimension parameters of the flaw

No	Inclination $\alpha/^\circ$	Coefficient of friction μ	No	Inclination $\alpha/^\circ$	Coefficient of friction μ
1-1	30	0.5	2-2	45	0
1-2	45	0.5	3-2	45	0.1
1-3	60	0.5	4-2	45	0.3
			5-2	45	0.7

Table 2 The parameter of material

Compressive strength /MPa	Tensile strength /MPa	Yonng's modulus /GPa	Possion's ratio
38.5	3.2	5.93	0.14

4.2 Modeling and Computing

Before the analysis of the program, we set appropriate loading steps and the number of iteration, which not only enables the convergent results, but also makes a good crack propagation path. During the meshing, the encryption (0.1mm*0.1mm) is made around the crack tip, while normal mesh (5mm*5mm) is chosen in other zones. After each converged load increment the crack propagation criterion is checked. If no crack growth happens, the current crack configuration remains unchanged and the next loading step is applied; otherwise a new crack segment will be inserted with some length (thought as the size of element). Subsequently, the process will continue with the next loading step (Fig. 4) [8].

4.3 Numerical results

The main findings from the modeling are as follows:

(1) Wing cracks are observed in all the models, which shows mode-I cracking is the main failure mode. Wing cracks appear first with a very short length at the tips of the initial crack, and then become wider and longer with the

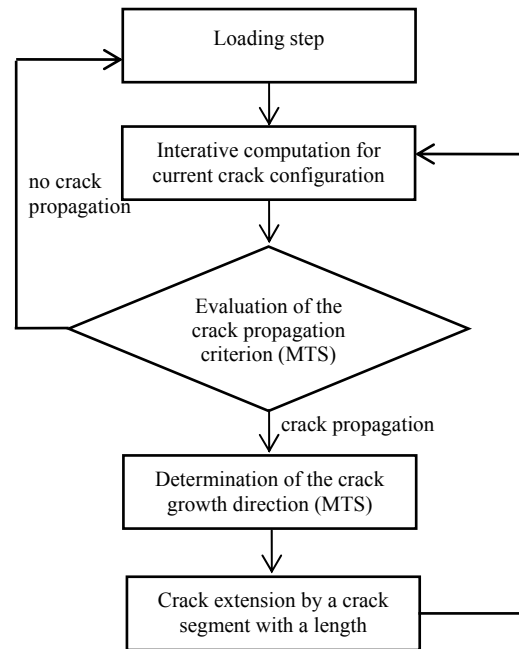


Fig. 4 Algorithm used for crack propagation analyses[8]

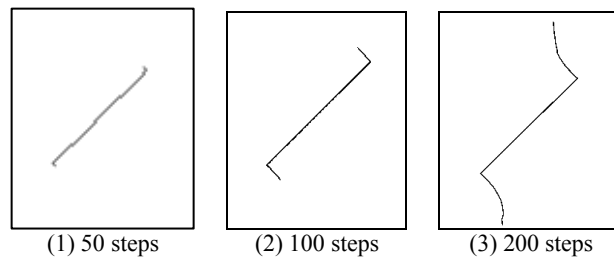


Fig. 5 The typical propagation path of the wing crack

load increasing, finally towards the direction of the compressive stress (Fig. 5). The path of wing crack seems to be similar to the hyperbola lines in mathematics, which are discussed in the previous papers of Yang who is one of this paper's authors.

(2) The crack in the infinite plate will completely keep open or close under the loading, while in the finite plate middle region maybe exist, which means the crack will close partly. Because of the complex in mathematics, it is difficult to obtain the analytical solution of the problem, and the phenomenon is observed in this modeling.

(3) The size has little effect in the vertical load increasing when the wing crack grows, so the model with fixed width and height is able to simulation the real results for different rock mass's situation.

(4) As the increase of the coefficient of the friction, the wing crack propagation will be slowly as the vertical load increase. Fig.7 also shows the crack faces will close when the length of wing crack reaches near 5mm. The curves extend mostly not as the line, which shows the friction over the crack face make the stress around the crack changed, thereby inhabit the propagation of the wing crack.

(5) The length of the wing crack increases nonlinearly as the vertical load increases, in details that increasing rate of crack length for vertical load increase at first and then decrease fast when the length of the wing crack reaches the critical value which means that the stress around the crack is changed due to the propagation of the crack. The initial load decreases as the increase of the inclination of the

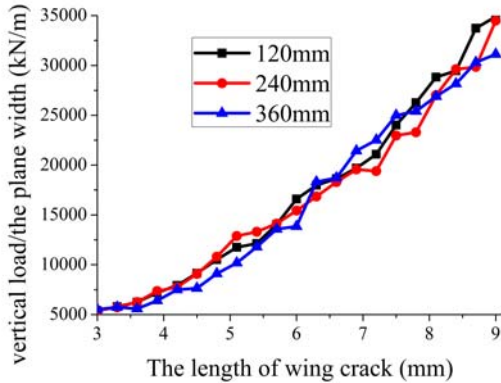


Fig. 6 Curve of the length of wing crack vs. vertical load/the plane width for $\mu=0.3$

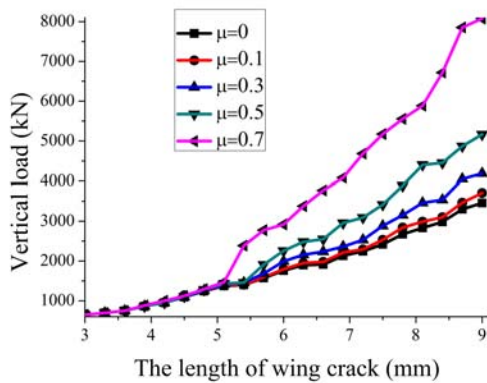


Fig. 7 Curve of the length of wing crack vs. vertical load for $\beta=45^\circ$

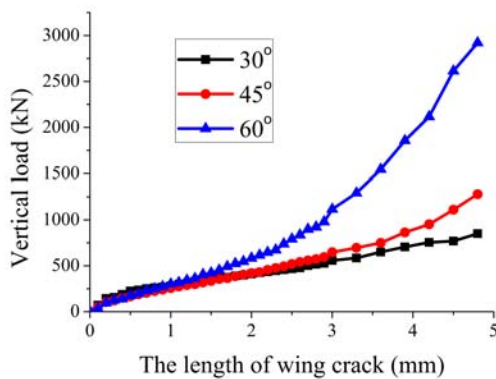


Fig. 8 Curve of the length of wing crack vs. vertical load for $\mu=0.5$

pre-set crack. The results in Fig. 8 show the difference of the inclination produce the different distribution of the normal and tangential stress.

5. CONCLUSIONS

The mechanism of crack propagation was studied using brittle material with the frictional contact under uniaxial expression and the relationship between the length of wing crack and vertical load was recorded and analyzed. A XFEM technique was used to simulate the propagation of wing cracks in the specimens, and the obtained results were compared with the laboratory test one [5], which shows they were very close to the experimental ones. It proves the accuracy and practicability of the above method in modeling the frictional contact behavior.

6. ACKNOWLEDGEMENTS

This research is supported by the NSFC (Grant No.50979013). The authors are grateful for these supports.

7. REFERENCES

- [1] Lu-xian, Li. & Tie-jun, Wang, "The extended finite element method and its applications," *Advances in Mechanics*, vol.35 (1), 2005, pp. 5-20.
- [2] Belytschko, T. & Black, T, "Elastic crack growth in finite elements with minimal remeshing," *Int. J. Numer. Meth. Eng.* vol.45 (5), 1999, pp. 601-620.
- [3] Moes, N., Dolbow, J. & Belytschko, T, "A finite element method for crack growth without remeshing," *Int. J. Numer. Meth. Eng.* vol.46 (1), 1999, pp. 131-150.
- [4] SIMULIA, ABAQUS 6.10: Analysis Users' Manual. 2010.
- [5] Shao-hua, G, "The experimental and theoretical investigation on fracture of rock-type materials under compressive loading," Ph.D. Thesis, 2003.
- [6] Dolbow, J., Moes, N. & Belytschko, T, "An extended finite element for modeling crack growth with frictional contact," *Computer Methods in Applied Mechanics and Engineering*, vol.190, 2001, pp. 6825-6846.
- [7] Yu-wen, D., Qing-wen, R. & Qin, S. "Extended finite element method of frictional contact problem," *Journal of Yangtze River Scientific Research Institute*, vol.26 (5), 2009, pp. 45-49.
- [8] Dumstorff, P. & Meschke, G. "Crack propagation in the framework of X-FEM-based structural analyses," *International Journal for Numerical and Analytical Methods in Geomechanics*. vol.31, 2007, pp. 239-259.

International Journal of GEOMATE, Sept., 2012, Vol. 3, No. 1 (Sl. No. 5), pp. 339-342

MS No. 1270 received August 30 2011, and reviewed under GEOMATE publication policies.

Copyright © 2012, International Journal of GEOMATE. All rights reserved, including the making of copies unless permission is obtained from the copyright proprietors. Pertinent discussion including authors' closure, if any, will be published in the Sept. 2013 if the discussion is received by March, 2013.

Corresponding Author: Jing-Cai Jiang